Eur Biophys J (1996) 25: 47–53

BIOPHYSICS LETTER

Alexander Mogilner · George Oster

The physics of lamellipodial protrusion

Received: 9 May 1996 / Accepted: 28 May 1996

Abstract Many cell movements appear to be driven by the polymerization of actin. Here we show how the force of polymerization can be generated by the thermal motions of the actin filaments near the sites of polymerization. We apply the model to explain the observations that the lamellipodial cytoskeleton is organized into an orthogonal network interspersed with filopodial protrusions, and that the protrusion of lamellipodia generally proceeds in the presence of a rearward cytoskeletal flow.

Introduction

Many types of cells spread thin veil-like sheets of cytoplasm, called lamellipodia, before them as they crawl over a substratum (Lee et al. 1993; Lee et al. 1994; Small 1994; Small et al. 1995; Theriot and Mitchison 1991). Of cells employing lamellipodia-driven locomotion, the fish keratocyte is one of the most studied. In this cell electron micrographs reveal that the lamellipodium is composed of a nearly orthogonal network of crosslinked actin filaments, interspersed with occasional parallel bundles that project to the leading edge (Cox et al. 1995; Small 1994; Small et al. 1995).

Peskin et al. formulated a theory to account for the force generated by the polymerization process itself when the filaments are rigid (Peskin et al. 1993). They proposed that the addition of subunits to the end of growing filaments rectified the Brownian motion of any diffusing object in front of the filament, and showed that this 'ratcheting' of diffusive motion could generate sufficient force to account for a number of motile phenomena. Here we generalize their model for rectified diffusion to describe the situation when the thermal fluctuations of either the actin fibers or membrane are significant. This extension provides a mechanical explanation for the protrusion of lamellipodia.

A. Mogilner
Department of Mathematics, University of California,
Davis, CA 95616, USA

G. Oster (✉)
Department of Molecular and Cellular Biology,
University of California, Berkeley, CA 94720-3112, USA

A model for lamellipodial extension

Figure 1 shows a schematic view of the filament and membrane arrangement we shall model. We treat the lamellipodium as a network of two populations of parallel, crosslinked fibers incident on the cytoplasmic face of the membrane at angles $\pm\theta$ measured from the membrane normal. A load force, f, is applied to the membrane over some area (Oliver et al. 1994). We assume that all fibers experience the same actin monomer concentration M, and so grow at the same rate in the same direction. We shall show that there is a critical angle θ_c at which the growth rate is fastest.

A filament bends much more easily than it compresses, and so the major mode of thermal motion for a fiber is a bending undulation. We shall treat only the bending fluctuations of the filament tips; i.e. the filament segment between the membrane and the first crosslink. We neglect the collective thermal modes of the actin meshwork, and consider it as a rigid anchor. We also neglect effects of electrostatic forces and cytoplasmic fluid flow.

We shall study two situations.

1. The membrane does not fluctuate sufficiently to permit intercalation of monomers onto the filament tips. We shall show that the thermal undulations of the filament tip can easily accommodate intercalation of the new monomers and drive protrusion. In this case there will be an optimal filament angle, θ_c, for fastest polymerization.
2. The membrane fluctuations are sufficient to permit intercalation, then the optimal filament angle will be $\theta = 0°$.

Case I: Membrane fluctuations are damped

We begin with the case when the membrane does not fluctuate sufficiently to permit polymerization. This will oc-

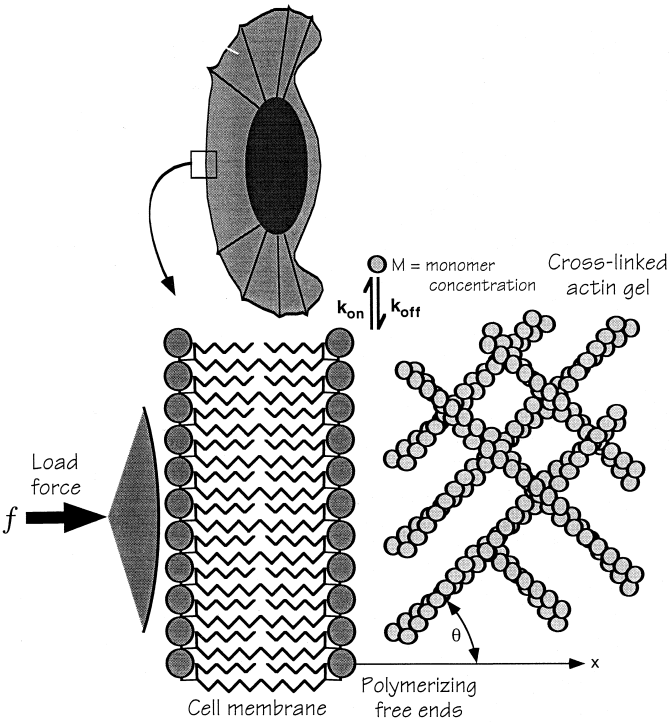

Fig. 1 The leading lamella of a migrating fibroblast is driven by a front of polymerizing actin filaments. The interface between the actin network and the membrane is shown schematically. The cross-linked actin network terminates near the membrane with free ends which impinge on the membrane at mean angles $\pm\theta$ measured from the membrane normal. The free ends are modeled by elastic filaments which are free to execute Brownian motion. If a thermal fluctuation is large enough and lasts long enough a monomer may intercalate onto the filament end with polymerization and depolymerization rates (k_{on} M) and k_{off}, respectively. The elongated filament is now slightly bent away from its mean equilibrium configuration so that its fluctuations exert an average elastic pressure against the membrane. Opposing the motion is a load force, *f*. The resistance to motion is the membrane tension, augmented by any external load applied, *f*, to the membrane

cur when the leading edge membrane is loaded with protein. There are compelling reasons to support this assumption. First, it is known that the actin polymerization that propels the bacterium *Listeria monocytogenes* through the cytoplasm of its host cell is triggered by the bacterial protein, ActA (Kocks and Cossart 1993; Kocks et al. 1993). When ActA is expressed in mammalian cells it stimulates actin-driven membrane ruffling and protrusion (Friederich et al. 1995). This strongly suggests that normal lamellipodial protrusion is stimulated by the action of analogous membrane associated proteins. Moreover, it is known that many membrane proteins localize to regions of high membrane curvature, especially at the tips of ruffles and lamellipodia (Odell and Oster 1993). In this situation, the effective diffusion coefficient characterizing membrane fluctuations would be defined by the proteins rather than the bilayer. Since the diffusion coefficients for membrane proteins are $D_p \sim 10^{-12} - 10^{-9}$ cm^2/s, it can be shown that these fluctuations would be too slow to support the intercalation of actin monomers onto the tips of the filaments. Below we treat the case where the density of membrane proteins is insufficient to damp the bilayer fluctuations sufficiently to inhibit polymerization

The filament can be considered as an elastic rod characterized by its persistence length, λ (Janmey et al. 1994).[1] The data on the numerical value of λ is variable, ranging between 0.5 μm (Kas et al. 1993) and 15 μm (Isambert et al. 1995). We feel that the lower measurements are more realistic for filaments at the leading edge, and so we shall use the value $\lambda \approx 1$ μm. The length of the free filament ends is of the order of the mean spacing between parallel fibers: $\ell \approx 30$ nm (calculated from (Small et al. 1995)).

We place our coordinate system on the leading edge membrane, measuring positive displacements perpendicularly inward from the membrane. Denote by x(t) the instantaneous distance of the tip from the membrane, and by y(t) the *equilibrium* (i. e. unbent) position of the filament tip at time t. For small displacements of the tip, it can be shown that the fluctuations of the tip are subject to an approximately harmonic restoring force $F_y(x) = -\kappa(x-y)$ (detailed calculations will be reported in Mogilner and Oster (1996). For small deflections, the corresponding angle-dependent effective elastic coefficient is $\kappa(\theta) \approx 4\lambda$ kT/$\ell^3 \sin^2\theta$. The effective diffusion coefficient associated with filament bending fluctuations is $D \approx K_B T/(6\pi\eta\ell) \approx 1-10$ μm^2/s, where η is the viscosity of the fluid phase of the cytoplasm, ~0.03 poise (Fushimi and Verkman 1991).

Let P(x, y, t) be the probability that a filament tip has fluctuated a distance (y − x) away from its equilibrium position y at time t. We describe the probability density for the location of the tip by an extension of the Fokker-Planck equation used in (Peskin et al. 1993):

$$\frac{\partial P}{\partial t} = \underbrace{D\frac{\partial^2 P}{\partial x^2}}_{\text{Diffusion of the tip}} - \underbrace{\frac{D}{k_B T}\frac{\partial}{\partial x}\left(F_y(x)P\right)}_{\text{Convection due to the elastic force exerted on the filament tip}} - \underbrace{V\frac{\partial P}{\partial y}}_{\text{Tip velocity relative to the membrane}} + \underbrace{\begin{cases} k_{on}M\left(P(x,y+\delta)-P(x,y)\right) \\ +k_{off}\left(P(x,y-\delta)-P(x,y)\right), & x>\delta \\ k_{on}MP(x,y+\delta)-k_{off}P(x,y), & x<\delta \end{cases}}_{\text{Polymerization at the filament tip}} \quad (1)$$

Here V is the protrusion velocity of the lamellipodium, T is the absolute temperature, k_B is Boltzmann's constant. Because actin filaments form a double helix, the intercalation distance, $\delta = 2.7$ nm, is one half size of the actin monomer. k_{on}, k_{off} are the polymerization and depolymerization rate constants, and M is the local concentration of polymerizable monomeric actin. The first term in Eq. (1) describes effective one-dimensional diffusion of the tip. The second term accounts for the motion of the tip towards

[1] The elastic bending modulus, B, of a filament is related to its persistence length by $B = \lambda k_B T$

its equilibrium position under the action of the elastic bending force. The third terms describes the motion of the tip with respect to the leading edge of the cell. The last term describes the polymerization kinetics of the filament, which depends on whether there is enough room between the tip and the membrane to intercalate a monomer (see Peskin et al. 1993 for more details).

We look for the asymptotically stable stationary solution of Eq. (1) on the half plane ($-\infty < y < \infty$, $x \geq 0$); the inequality holds because the membrane is impenetrable. The probability, P, is subject to the normalization condition and to zero flux boundary conditions at the membrane. Under physically reasonable conditions, the third and forth terms can be treated as small perturbations on the first two terms. That is, the time scale for tip fluctuations is much smaller than that for polymerization and protrusion. The stationary solution for Eq. (1) was obtained using a multiscale perturbation analysis, which yields the following expression for the protrusion velocity:

$$V \approx \delta \cos\theta \left[k_{on}\, M \hat{p}(\theta, y_0) - k_{off} \right] \tag{2}$$

where

$$\hat{p}(\theta, q_0) = \frac{\int_{\delta\cos\theta}^{\infty} \exp\left(-\kappa (x - y_0)^2 / 2 k_B T\right) dx}{\sum_{0}^{\infty} \exp\left(-\kappa (x - y_0)^2 / 2 k_B T\right) dx} \tag{3}$$

Equation (2) resembles the expression for the free polymerization velocity, $V_p = \delta(k_{on}M - k_{off})$, where δ is modified to ($\delta \cos\theta$) to account for the angle of the polymer to the membrane, and $\hat{p}(\theta, y_0)$ is the probability of a gap of sufficient size and duration to permit intercalation of a monomer. The expression for $\hat{p}(\theta, y_0)$ given by Eq. (3) depends on y_0, the asymptotic equilibrium distance of the tip from the membrane, which can be found as follows. The force, f, exerted by a fluctuating filament against the load – the main source of which is the applied resistance of a microneedle (Oliver et al. 1994) – is computed from the elastic free energy of a semi-stiff rod (Landau and Lifshitz 1970 a):

$$f \approx k_B T \frac{\exp\left(-\frac{\kappa y_0^2}{2 k_B T}\right)}{\int_0^{\infty} \exp\left(-\frac{\kappa (x - y_0)^2}{2 k_B T}\right) dx} \tag{4}$$

Equation (4) also depends on y_0; eliminating y_0 parametrically from formulae (2–4), we obtain an expression for the protrusion velocity V as a function of the variables f and θ for fixed ℓ, λ, and δ. V(f, θ) is plotted in Fig. 2.

For filament tips longer than $\ell \sim 0.1$ μm, a flexible filament (i.e. $\lambda \sim 1$ μm) can grow even if it approaches the load perpendicularly, since thermal motions can bend it easily to allow intercalation of monomers. A stiffer filament must approach the load at an angle to the normal to permit intercalation since the probability of a sufficient gap increases with the angle of incidence (the effective elastic coefficient is smaller). For the same reason, a larger load force favors the growth of filaments at larger angles. Clearly, protrusion ceases where the filament is parallel to the membrane ($\theta \to \pi/2$); therefore, a critical angle, θ_c, exists at which the protrusion velocity is maximal. This critical angle depends on the load force as well as the filament stiffness. We have derived an approximate expression of the optimal angle in the case when the only load is the membrane tensions ($\sigma \sim 3.5 \times 10^{-2}$ pN/nm (Cevc and Marsh 1987)):

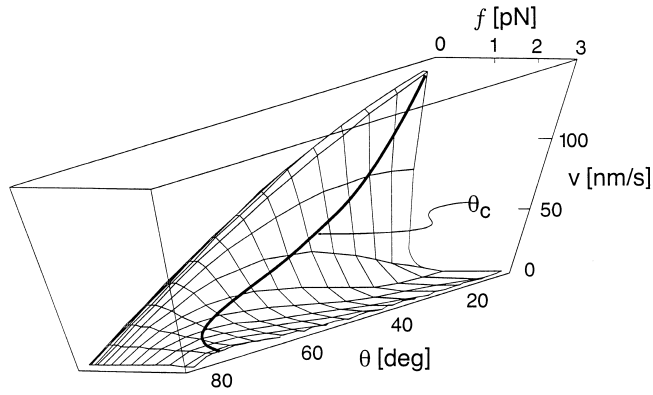

Fig. 2 Lamellipodial velocity in nanometers per second as a function of load, f, in pN, and filament incidence angle, θ, in degrees for fixed length, ℓ, and persistence length, λ, given in Table 1. The critical angle, θ_c, for fastest growth depends on the load; the trajectory of θ_c is shown on the v(f, θ) surface connecting the loci of maximum velocity at each load. v(θ_c) corresponds to a typical velocity of about 0.1 μm/s providing we assume a monomer concentration of about 10 μM. While this is higher than cytoplasmic concentrations, the presence of recruiting proteins analogous to ActA in *Listeria* could easily raise the local concentration of polymerization-competent monomers to this level (Cooper 1991; Theriot 1994). The optimal angle θ_c, is an increasing function of the load force. When the load force is large enough, the velocity passes through a maximum at θ_c. The figure was computed from the load-velocity expressions (2–4). The parameter values employed in the computations are given in Table 1

$$\theta_c \approx \tan^{-1}\left(\frac{2\delta\sqrt{\lambda}}{\ell^{3/2}}\right) \tag{5}$$

Using the parameter values given in Table 1 we find $\theta_c \approx 48°$. This is close to the angle observed by Small for lamellipodia in fish keratocytes (Small et al. 1995). At such angle and force the derived protrusion velocity is in the observed range of 0.1–1 μm/s, (Lee et al. 1993).

Finally, the model predicts a stall force for a single filament as

$$f_s \approx \frac{2 k_B T}{\ell} \sqrt{\frac{\lambda}{\delta}} \tag{6}$$

Using the parameters in Table 1, we obtain $f_s \sim 5$ pN. Using the micrographs of Small (1995) to estimate the dimensions of a lamellipod and the total number of filaments, we arrive at a total stall force $f_s \sim 10^3 - 10^4$ pN; this compares favorably with the experimental value of 4.5×10^4 pN reported by Oliver et al. (1994).

Table 1 Parameter values

Parameter	Value	Reference
δ = effective half monomer size	2.7 nm	(Pollard 1986)
k_{on} = polymerization rate	11 s^{-1} μM^{-1}	(Pollard 1986)
k_{off} = depolymerization rate	1 s^{-1}	(Pollard 1986)
M = monomer concentration	10 μM	(Marchand et al. 1995)
λ = filament persistence length	1 μm	(Kas et al. 1993)
ℓ = length of filaments tips	30 nm	(Small et al. 1995)
H = thickness of lamellipod	200 nm	(Lee et al. 1993)
A = cross-sectional area of lamellipod	0.2 μm^2	(Oliver et al. 1994)
k_BT	4.1 pN×nm	
σ = membrane surface tension	0.035 pN/nm	(Cevc and Marsh 1987)
η = viscosity of the fluid part of the cytoplasm	0.03 poise	(Fushimi and Verkman 1991)
B_m = bending stiffness of the membrane	(5 – 50) k_BT	(Bo and Waugh 1989; Evans and Yeung 1989)

Case 2: Membrane fluctuations are significant

When the concentration of protein in the leading edge membrane is low, membrane fluctuations are sufficient to permit intercalation of monomers. We consider the case when the transmembrane protein density is not sufficient to dampen membrane fluctuations. Let us consider free protrusion when the load force f is given by the membrane surface tension. The corresponding pressure $P \sim 2\sigma/H \approx 3.5 \times 10^{-4}$ pN/nm^2, where H ≈ 200 nm is the thickness of lamellipodia (Lee et al. 1993). The average amplitude of membrane fluctuations, h, is related to the pressure on the membrane by the following asymptotic formulae (Sackmann 1996): $P \sim (k_BT)^2/(B_m h^3)$ if $\sigma \ll k_BT/h^2$. In the situation under study here amplitudes are of the order of a few nm, and the inequality holds. Here $B_m \approx 5-50\ k_BT$ is the membrane bending stiffness (Bo and Waugh 1989; Evans and Yeung 1989). We estimate the average amplitude of membrane fluctuations as $h \sim ((k_BT)^2/(B_mP))^{1/3} \approx 7-15$ nm. This is much larger than the minimal gap needed for intercalation of an actin monomer. The wavelength of the fluctuations corresponding to these amplitudes is $L \sim h\sqrt{B_m / k_B T} \sim (10-100)$ nm (Sackmann 1996), and the corresponding effective diffusion coefficient can be estimated as $D_m \sim k_BT/(6\pi\eta L) \sim 1-10\ \mu m^2/s$ (Leibler et al. 1987). These fluctuations would be fast and large enough to provide an effective polymerization velocity equal to the ideal polymerization velocity $V_p \approx 0.3$ μm/s (for the parameter values given in Table 1).

In this situation, the angle corresponding the fastest filament growth, θ_c, is normal to the membrane since the filaments do not need to bend in order to polymerize. This situation can arise when a fluctuation in the density of membrane proteins produces a local region where the bilayer fluctuations permit intercalation of monomers onto the filament tips. In this region the filaments perpendicular to the membrane will grow fastest. Also, if the crosslinking density at the tip falls so that filament tip length exceeds approximately 150 nm, then the filaments become flexible enough to intercalate monomers even when θ_c=90°. In either case, we interpret the nucleation of parallel crosslinked filament bundles as the beginning stages of filopod formation. On the basis of this picture, we expect that the membrane region between filopodia will be characterized by increased membrane tension and protein loading. Thus the regions between the filopodia will fill in via lamellipod growth, like the web on a duck's foot.

We can estimate the stall force in this case as follows. The load pressure sufficient to suppress the amplitude of membrane fluctuations to about δ is $P_s \sim (k_BT)^2/(B_m\delta^3)$. The corresponding stall force is $f_s \sim (k_BT)^2A/(B_m\delta^3) \approx 10^3 - 5 \times 10^4$ pN, where A ~ 0.2 μm^2 is the projected cross-sectional area of the lamellipod. This estimate is again of the same magnitude as the force reported in (Oliver et al. 1995).

Centripetal flow during lamellipodial protrusion

During lamellipodial protrusion, particles and ruffles on the dorsal surface of the lamella move centripetally towards the perinuclear area. This retrograde, or centripetal flow of lamellar substance accompanies cell migration, implying there is a counter-flow of material in the lamellipod (Sheetz 1994; Small 1994; Stossel 1993; Theriot and Mitchison 1991). Fast centripetal flow of up to 100 nm/s is observed in neural growth cone lamellae (Lin and Forscher 1995). In fibroblasts, where a gradient in lamella density from the leading edge to the perinuclear region is substantial, the centripetal flow is fast, while in keratocytes, where the gradient is small, centripetal flow is slow (Sheetz 1994).

To model centripetal flow we assume that polymerization of actin takes place mainly at the leading edge. Before crosslinking, the free ends of actin fibers must be stress free. Crosslinking permits stress to develop due to the entropic motions of the chains between the cross-links. Back from the leading edge, filaments start to disassemble, either spontaneously or from the action of solation proteins, or both. This causes a gradual increase in the distances between neighboring crosslinks or entanglement loci. The average distances between such points anywhere in the lamella are much smaller than the lowest estimates for the persistent length of actin. Therefore, filaments must be treated as elastic semistiff rods, rather than entropically flexible threads. Due to thermal writhing, when filaments

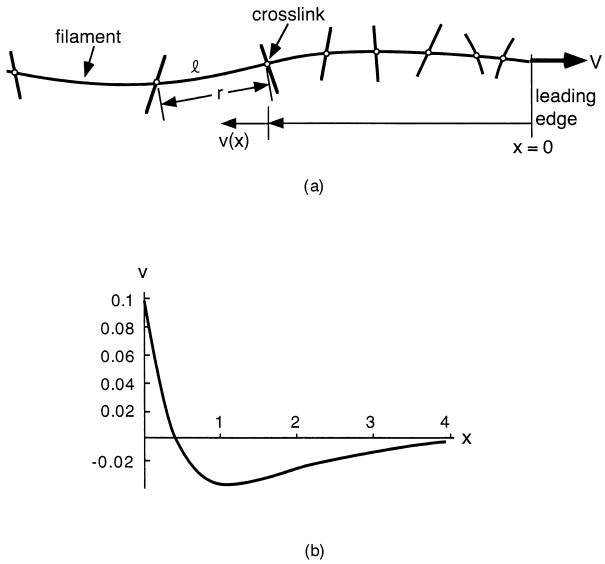

Fig. 3 **a** A single filament crosslinked into the cortical network. Polymerization driven protrusion takes place at the tip with constant velocity V. We place our coordinate system at the leading edge and measure x backwards from the tip. Rather than crosslink density, we use $r(x, t)$, the distribution of distances between the crosslinks, and $\ell(x, t)$, the distribution of the filament lengths between the crosslinks, $v(x)$ is the retrograde velocity field. **b** The normalized retrograde velocity field, v/V, as a function of the dimensionless proximal distance, $x\,\mu/V$. Note that the retrograde velocity eventually goes negative, as is observed sometimes in locomoting keratocytes

are polymerized and cross-linked in a stress-free state, the average distance between cross-links is slightly smaller than the average fiber length between cross-links. When the distance between cross-links grows due to partial solation of the network (due to filament severing, crosslink dissolution and filament depolymerization), it is easy to show that the equilibrium distance between cross-links decreases still more, and the consequent stress in the filaments strains the actin meshwork. So, depolymeriziation causes an entropic, contractile stress.

We can estimate the magnitude of the solation induced network stress as follows. Focus attention on a single filament, as shown in Fig. 3a. The equilibrium distance between the ends of a thermally fluctuating elastic rod of length ℓ is (Landau and Lifshitz 1970b):

$$r_{eq} \approx \ell(1 - \ell/6\lambda), \tag{7}$$

where $\lambda \gg \ell$ is the persistence length. The force, F, to change the distance between the ends of the rod from its equilibrium distance r_{eq} to r is (MacKintosh et al. 1995):

$$F \approx \left(90\frac{k_B T\lambda^2}{\ell^4}\right)(r - r_{eq}) \tag{8}$$

The corresponding contractile force induced in the rod when a single crosslink is removed is $F \sim 2\ k_B T\lambda/\ell^2 \approx 8$ pN.[2]

[2] A better estimate based on a more realistic model is 5 pN for an entire fiber (Mogilner and Oster, in preparation)

As the network density decreases with disassembly, the stress rises; therefore, solation of the network generates a stress gradient which increases from the leading edge proximally towards the cell center. This stress gradient is sufficient to drive the creeping rearward motion of the cortical actin network against the resistance due to viscous drag of cytoplasm and the breaking of transmembrane bonds with the substratum. Thus the net forward motion of the lamellipod will be determined by the balance of protrusive and centripetal forces. We can construct a simplified, 1-dimensional model of a longitudinal cross-section of the lamellipod as follows.

We focus our attention on a single filament, and place our coordinate system at the tip of the lamellipod, as shown in Fig. 3a. Let x denote the proximal distance from the leading edge along the filament and write balance equations for the crosslinking nodes and for the axial stress in the lamellipod. It is convenient to characterize the network by the distribution of distances between crosslinks, denoted by $r(x, t)$, rather than the crosslinks themselves. Denote the length distribution of the filaments between crosslinks by $\ell(x, t)$, so that the local strain is $(r - r_{eq}(\ell))$. The evolution of these distributions is governed by the following balance equations:

$$\frac{\partial r}{\partial t} = -(V + v)\frac{\partial r}{\partial x} + \mu r + r\frac{\partial v}{\partial x} \tag{9}$$

$$\frac{\partial \ell}{\partial t} = -\frac{\partial}{\partial x}[(V + v)\ell] + \mu\ell \tag{10}$$

where the centripetal velocity, $v(x)$, is given by:

$$v(x) \approx \left(90\frac{k_B T\lambda^2}{\zeta}\right) r\frac{d}{dx}\left[\frac{r - r_{eq}}{\ell^4}\right] \tag{11}$$

Here ζ is the effective viscous friction coefficient for movement of the network through cytoplasm (which we consider constant here for the sake of simplicity). V is the polymerization velocity and μ is a rate of cross-link dissociation. The first terms in each equation are the convective fluxes and the second terms account for the decrease in node density due to solation (loss of nodes). The last term in Eq. (9) accounts for the change in r due to the difference in velocity of adjacent nodes. We shall consider the lamellipod of the fish keratocyte where the centripetal velocity is small compared to the protrusion velocity: $v/V \ll 1$. In this situation we can use perturbation theory to find the asymptotically stable stationary solution. In the first approximation, the stationary distributions of r and ℓ are given simply by

$$\begin{aligned} -V\frac{\partial r}{\partial x} + \mu r &= 0 \\ -V\frac{\partial \ell}{\partial x} + \mu\ell &= 0 \end{aligned} \tag{12}$$

The boundary conditions specify the mesh size at the leading edge, $r(0) = r_0$, and the condition that the leading node is strain free: $\ell(0) = \ell_0$, where r_0 and ℓ_0 are related by

Eq. (7). The solution to Eq. (12) is

$$\begin{pmatrix} r \\ \ell \end{pmatrix} = \begin{pmatrix} r_0 \\ \ell_0 \end{pmatrix} e^{\mu x / V} \tag{13}$$

which yields the centripetal velocity field defined in the expression (11), v (x)

$$v(x) \approx \left(15 \frac{k_B T \lambda \mu}{\zeta \ell_0 V} \right) (3e^{-2\mu x / V} - 2e^{-\mu x / V}) \tag{14}$$

v(x) is plotted in Fig. 3 b. The corresponding filament density, $n(x) \sim 1/r(x)$, is in qualitative accordance with the observations of Small on the distribution of actin filaments in locomoting keratocytes (Small et al. 1995). Note that, at large distances from the leading edge, the network velocity reverses (Sheetz 1994).

Discussion

By extending the polymerization ratchet model of Peskin, et al. (1993) to permit flexible filaments we have been able to construct a more complete picture of the physics of force generation at the leading edge of the lamellipodium. The model predicts the following features of lamellipodial protrusion:

– The force and velocity of protrusion due to actin polymerization.
– The orthogonal network geometry observed in keratocyte lamellipodia.
– The interspersion of parallel bundled actin filaments which may nucleate filopodia.
– Centripetal flow of the network that accompanies protrusion.

In addition, the elastic ratchet model provides an interpretation for other features of lamellipodial driven cell motion. For example, increasing external osmolarity tends to arrest cell protrusion (Trinkaus 1984). We interpret this in the context of the model as follows. External osmolytes will dehydrate the region near the leading edge causing the membrane to 'shrink-wrap' the free filament tips. This arrests polymerization and stops protrusion. If the cell is not strongly adherent to the substratum, the lamellipod may retract due to the stress gradient driven retraction force; if the tip bends away from the substratum, a ruffle commences. A similar effect can be brought about by introducing agents such as cytocholasin that inhibit actin polymerization (Forscher and Lin 1995).

We note that there are alternative interpretations of the filament geometry in the leading lamella. For example, actin binding proteins, such as profilin, may favor binding of actin filaments which collide normal to each other (Hartwig 1992). It is feasible that such proteins can nucleate new filaments from existing filaments near the membrane, which could generate the observed orthogonal architecture (Civelekoglu and Edelstein-Keshet 1994). In fact, if this hypothesis about angular dependent binding of actin is true, then it is possible that filaments are nucleated in the direction given by the fastest growth condition given here, and the "frozen" into orthogonal order by actin-binding proteins.

Finally, we expect that the elastic ratchet model applies to other polymerization driven phenomena such as phagocytosis (Swanson and Baer 1995), inductopodia (Forscher et al. 1992) and microtubule deformation of liposomes (Fygenson 1995; Miyamoto and Hotani 1988; Miyata and Hotani 1992), platelet activation (Winojur and Hartwig 1995), the propulsion of certain pathogenic bacteria, such as *Listeria monocytogenes*, through the cytoplasm of their hosts (Marchand et al. 1995; Zhukarev et al. 1995), and the infective protrusions generated by certain viruses, such as vaccinia (Cudmore et al. 1995). Nor is the model restricted to systems driven by actin polymerization. Nematode sperm extend a lamellipodium and crawl by assembling not actin, but an unrelated protein called major sperm protein (Roberts and King 1991; Roberts and Stewart 1995). These lamellipodia resemble in most aspects those of mammalian cells and we believe that the underlying physics is the same.

Acknowledgements AM was supported by the Program in Mathematics and Molecular Biology, University of California, Berkeley. GO was supported by National Science Foundation Grant DMS 9220719. The authors would like to thank Julie Theriot, Paul Janmey, Casey Cunningham, John Hartwig, and Charles Peskin for valuable comments and criticism.

References

Bo L, Waugh RE (1989) Determination of bilayer membrane bending stiffness by tether formation from giant thin-walled vesicles. Biophys J 55: 509 – 517
Cevc G, Marsh D (1987) Phospholipid Bilayers. Wiley, New York
Civelekoglu G, Edelstein-Keshet L (1994) Modelling the dynamics of F-actin in the cell. Bull Math Biol 56: 587 – 616
Cooper JA (1991) The role of actin polymerization in cell motility. Ann Rev Physiol 53: 585 – 605
Cox D, Ridsdale A, Condeelins J, Hartwig J (1995) Genetic deletion of ABP-120 alters the three-dimensional organization of actin filaments in *Dictyostelium* pseudopods. J Cell Biol 128: 819 – 835
Cudmore S, Cossart P, Griffiths G, Way M (1995) Actin-based motility of vaccinia virus. Nature 378: 636 – 638
Evans E, Yeung A (1989) Apparent viscosity and cortical tension of blood granulocytes determined by micropipet aspiration. Biophys J 56: 161 – 168
Forscher P, Lin C (1995) Steady state processes underlying neuronal growth cone motility. Molec Biol Cell 6: 229 – 232
Forscher P, Lin CH, Thompson C (1992) Inductopodia: A novel form of stimulus-evoked growth cone motility involving site directed actin filament assembly. Nature 357: 515 – 518
Friederich E, Gouin E, Hellio R, Kocks C, Cossart P, Louvard D (1995) Targeting of Listeria monocytogenes ActA protein to the plasma membrane as a tool to dissect both actin-based cell morphogenesis and ActA function. Embo J 14: 2731 – 2744
Fushimi K, Verkman AS (1991) Low viscosity in the aqueous domain of cell cytoplasm measured by picosecond polarization microfluorimetry. J Cell Biol 112: 719 – 725
Fygenson D (1995) Microtubules: the rhythm of assembly and the evolution of form Ph. D. Thesis. Princeton University, Princeton
Hartwig JH (1992) Mechanisms of actin rearranagments mediating platelet activation. J Cell Biol 118: 1421 – 1442

Isambert H, Venier P, Maggs A, Fattoum A, Kassab R, Pantaloni D, Carlier M-F (1995) Flexibility of actin filaments derived from thermal fluctuations. Effect of bound nucleotide, phalloidin, and muscle regulatory proteins. J Biol Chem 270: 11437 – 11444

Janmey PA, Hvidt S, Kas J, Lerche D, Maggs A, Sackmann E, Schliwa M, Stossel TP (1994) The mechanical properties of actin gels. Elastic modulus and filament motions. J Biol Chem 269: 503 – 32513

Kas J, Strey H, Barmann M, Sackmann E (1993) Direct measurement of the wave-vector-dependent bending stiffness of freely flickering actin filaments. Europhys Lett 21: 865 – 870

Kocks C, Cossart P (1993) Directional actin assembly by Listeria monocytogenes at the site of polar surface expression of the actA gene product involving the actin-bundling protein plastin (fimbrin). Infect Agents Dis 2: 207 – 209

Kocks C, Hellio R, Grounon P, Ohayon H, Cossart P (1993) Polarized distribution of Listeria monocytogenes surface protein ActA at the site of directional actin assembly. J Cell Sci 105: 699 – 710

Landau L, Lifshitz E (1970 b) The Theory of Elasticity, 2nd edn. Pergamon, London

Landau L, Lifshitz E (1970 a) Statistical Physics, 2nd edn. Pergamon, London

Lee J, Ishihara A, Theriot JA, Jacobson K (1993) Principles of locomotion for simple-shaped cells. Nature 362: 467 – 471

Lee J, Leonard M, Oliver T, Ishihara A, Jacobson K (1994) Traction forces generated by locomoting keratocytes. J Cell Biol 127: 1957 – 1964

Leibler S, Lipowsky R, Peliti L (1987) Curvature and fluctuations of amphiphilic membranes. In: Meunier J, et al. (eds) Physics of Amphiphilic Layers, vol 21. Springer-Verlag, New York, pp 74 – 79

Lin C, Forscher P (1995) Growth cone advance is inversely proportional to retrograde F-actin flow. Neuron 14: 763 – 771

MacKintosh F, Kas J, Janmey P (1995) Elasticity of semiflexible biopolymer networks. Phys Rev Lett 75: 4425 – 4429

Marchand J-B, Moreau P, Paoletti A, Cossart P, Carlier M-F, Pantoloni D (1995) Actin-based movement of Listeria monocytogenes: Actin assembly results from the local maintenance of uncapped filament barbed ends at the bacterium surface. J Cell Biol 130: 331 – 343

Miyamoto H, Hotani H (1988) Polymerization of microtubules within liposomes produces morphological change of their shapes. In: Hotani H (ed) Taniguchi International Symposium on Dynamics of Microtubules, vol 14. The Taniguchi Foundation, Taniguchi, Japan, pp 220 – 242

Miyata H, Hotani H (1992) Morphological changes in liposomes caused by polymerization of encapsulated actin and spontaneous formation of actin bundles. Proc Natl Acad Sci 89: 11547 – 11551

Mogilner A, Oster G (1996) Cell motility driven by actin polymerization. Biophys J (in press)

Odell E, Oster G (1993) Curvature segregation of proteins in the Golgi. In: Goldstein B, Wofcy C (eds) Some Mathematical Problems in Biology, vol 24. American Mathematical Society, Providence, RI, pp 23 – 36

Oliver T, Dembo M, Jacobson K (1995) Traction forces in locomoting cells. Cell Motil Cytoskeleton 31: 225 – 240

Oliver T, Lee J, Jacobson K (1994) Forces exerted by locomoting cells. Semin Cell Biol 5: 139 – 147

Peskin C, Odell G, Oster G (1993) Cellular motions and thermal fluctuations: The brownian ratchet. Biophys J 65: 316 – 324

Pollard T (1986) Rate constants for the reactions of ATP- and ADP-actin with the ends of actin filaments. J Cell Biol 103: 2747 – 2754

Roberts T, King K (1991) Centripetal flow and directed reassembly of the major sperm protein (MSP) cytoskeleton in the amoeboid sperm of the nematode, *Ascaris*. Cell Motil Cytoskeleton 20: 228 – 241

Roberts T, Stewart M (1995) Nematode sperm locomotion. Curr Opin Cell Biol 7: 13 – 17

Sackmann E (1996) Supported membranes: scientific and practical applications. Science 271: 43 – 48

Sheetz M (1994) Cell migration by graded attachment to substrates and contraction. Semin Cell Biol 5: 149 – 155

Small JV (1994) Lamellipodia architecture: actin filament turnover and the lateral flow of actin filaments during motility. Semin Cell Biol 5: 157 – 163

Small JV, Herzog M, Anderson K (1995) Actin filament organization in the fish keratocyte lamellipodium. J Cell Biol 129: 1275 – 1286

Stossel T (1993) On the crawling of animal cells. Science 260: 1086 – 1094

Swanson JA, Baer SC (1995) Phagocytosis by zippers and triggers. Trends in Cell Biol 5: 89 – 93

Theriot JA (1994) Actin filament dynamics in cell motility. Adv Exp Med Biol 358: 133 – 145

Theriot JA, Mitchison T (1991) Actin microfilament dynamics in locomoting cells. Nature 352: 126 – 131

Trinkaus J (1984) Cells into Organs: Forces that Shape the Embryo, 2nd edn. Prentice Hall, Englewood Cliffs, NJ

Winojur R, Hartwig J (1995) Mechanism of shape change in chilled human platelets. Blood 85: 1736 – 1804

Zhukarev V, Ashton F, Sanger J, Sanger J, Shumann H (1995) Organization and structure of actin filament bundles in Listeria-infected cells. Cell Motil Cytoskeleton 30: 229 – 246